HHS Public Access

Author manuscript

Ophthalmic Genet. Author manuscript; available in PMC 2016 March 03.

Published in final edited form as:

Ophthalmic Genet. 2015 June ; 36(2): 113–122. doi:10.3109/13816810.2013.841962.

Bilateral Concordance of the Fundus Hyperautofluorescent Ring in Typical Retinitis Pigmentosa Patients

Tharikarn Sujirakul[1,2], **Richard Davis**[1], **Deniz Erol**[1], **Lijuan Zhang**[1], **Giuseppe Schillizzi**[1], **Leticia Royo-Dujardin**[1], **Sherry Shen**[1,3], and **Stephen Tsang**[1,4]

[1]Department of Ophthalmology, Columbia University, New York, NY, USA [2]Department of Ophthalmology, Ramathibodi Hospital, Mahidol University, Bangkok, Thailand [3]College of Physicians & Surgeons, Columbia University, New York, NY, USA [4]Department of Pathology and Cell Biology, Columbia University, New York, NY, USA

Abstract

Background—It has long been assumed that in retinitis pigmentosa, disease presentation and progression are symmetrical. This study investigated whether hyperautofluorescent ring size, one known marker of disease progression, is symmetrical in typical RP patients.

Materials and Methods—A total of 88 patients with typical retinitis pigmentosa were enrolled in the study. Each presented with a hyperautofluorescent ring when imaged at baseline with fundus autofluorescence (AF). Vertical and horizontal diameters were analyzed according to mode of inheritance and age group. Seven of 88 patients had data missing in one eye and were excluded from further analysis.

Results—There was no significant relationship between hyperautofluorescent ring diameter and inheritance mode. There was a tendency toward smaller ring size with age and 3.7% of subjects displayed marked asymmetry in ring size between right and left eyes, although their electroretinogram results did not differ. Overall, when patients were considered as a group, there was a high correlation between right and left eyes' horizontal and vertical diameters ($r = 0.99$, $p<0.0001$; $r = 0.98$, $p<0.0001$). Comparing individual patients' eyes, and accounting for measurement error, a smaller majority of patients displayed symmetry of the hyperautofluorescent ring in both dimensions (85.7% in the vertical dimension, 87.3% in the horizontal dimension).

Correspondence: Stephen H. Tsang, MD, PhD, Department of Ophthalmology, Columbia University Medical Center, New York, NY, USA. Tel: +1 212 342 1186. sht2@columbia.edu.

DECLARATION OF INTEREST

The authors report no conflicts of interest. The authors alone are responsible for the content and writing of the paper.

Tharikarn Sujirakul was supported by Foundation Fighting Blindness grant CF-CL-0613-0614-COLU. The Edward and Shirlee Brown Glaucoma Laboratory is supported by NIH core grants 5P30CA013696 and P30EY019007, Research to Prevent Blindness (R01EY018213), the Research to Prevent Blindness Physician-Scientist Award, the Barbara and Donald Jonas Family Fund, the Schneeweiss Stem Cell Fund, New York State (N09G-302), the Foundation Fighting Blindness New York Regional Research Center Grant (C-NY05-0705-0312). Financial support for Sherry Shen was provided by NHLBI (5T35HL007616-3) and Fight for Sight. S. H. Tsang is a Fellow of the Burroughs-Wellcome Program in Biomedical Sciences, and has been supported by the Bernard Becker Association of University Professors in Ophthalmology Research to Prevent Blindness Award, the Dennis W. Jahnigen Award of the American Geriatrics Society, the Joel Hoffman Fund, Gale and Richard Siegel Stem Cell Fund, Charles Culpeper Scholarship, Irma T. Hirschl Charitable Trust, Bernard and Anne Spitzer Stem Cell Fund, and Professor Gertrude Rothschild Stem Cell Foundation.

Conclusion—This study confirmed the highly symmetrical nature of the hyperautofluorescent ring in RP patients, except in a small subgroup. AF results, which provide less variability per image, and are consistently interpreted between different observers, may be a more sensitive and reliable method for testing symmetry than many functional tests.

Keywords

Fundus autofluorescence; hyperautofluorescent ring; retinitis pigmentosa; symmetry and asymmetry

INTRODUCTION

Retinitis pigmentosa (RP) is a group of inherited retinal diseases characterized by photoreceptor degeneration. Rods are primarily affected, followed by cones. This condition can lead to blindness in the advanced stages of disease, when central cones become involved.[1] RP is usually considered a bilateral disease that appears to affect both eyes in a highly symmetrical fashion except in rare instances, such as in unilateral RP. The most common cause of asymmetrical RP cases is lyonization, or random x-inactivation, seen in X-linked RP female carriers.[2–4] However unilateral RP has been reported in a patient with an RP1 germline mutation.[5] Other causes of asymmetrical pigmentary retinopathy that could mimic asymmetrical or unilateral RP include infection, inflammation, intraocular foreign body and trauma.[6–9] All in all, these have typically been assumed to be exceptions to a general rule of symmetry, or bilateral concordance.

Despite the long-term assumption that RP is a symmetrical condition, there are only a few published studies that have been undertaken to describe this symmetry, beginning with Jules Gonin's pioneering case studies in 1901. In 1963, Biro and colleagues reported the symmetrical development of pigmentation as a specific feature in RP.[10] In 1979, Massof and colleagues reported bilateral visual field symmetry in RP patients. Theirs was the largest study to date, involving 60 typical RP patients who underwent functional testing.[11] With the advent of gene therapy and stem cell treatments, it has become more and more relevant to establish whether bilateral concordance is the norm. The eye's utility as a proving ground for these therapies rests on an assumption of symmetry.[12–14]

In recent years, new imaging techniques have been developed that would allow for these investigations to take place at the structural level. Fundus autofluorescence (AF), commonly used in the diagnosis and follow-up in patients with retinitis pigmentosa, can be used to identify disease progression over time.[15–20] AF has the ability to image structural features such as the hyperautofluorescent ring, seen in 59–94% of RP patients including in simplex and syndromic RP, and common in every inheritance pattern.[21–23] This ring is a structural indicator for RP progression and has been reported to correlate well with other structural and functional assessments, such as optical coherence tomography (OCT), pattern electroretinograms (ERG), multifocal ERGs, microperimetry and visual fields.[24–29]

The origins of the AF signal remain uncertain, but it is believed to be caused by accumulation of lipofuscin due to the phagocytosis of photoreceptor outer segments in the retinal pigment epithelium. It is likely that abnormal hyperautofluorescence comes either

from the increased accumulation of lipofuscin related to increased outer segment dysgenesis in RP patients, or from increased fluorescence transmission due to the loss of the ellipsoid line and thinning of the outer plexiform layer.[30–33] In this study, hyperautofluorescent ring size was used as an index of disease progression. Ring size was calculated by measuring the diameter of the ring, both vertically and horizontally, and then comparing left and right eyes. Overall, this was the first study to use structural imaging to examine whether RP eyes show true bilateral concordance.

METHODS

Subjects

A total of 88 typical RP patients from the electrodiagnostics clinic at Columbia University's Harkness Eye Institute who manifested a hyperautofluorescent ring or arc during fundus autofluorescence imaging on their first visit participated in this retrospective cross-sectional study. All subjects gave their consent. No cases of unilateral RP, paravenous RP, or X-linked RP in female patients were included in the study. Baseline and hyperautofluorescent ring were evaluated. Out of the initial 88 RP patients, seven were later excluded from symmetrical analyses due to missing data in one eye, or a condition that prevented fundus autofluorescence imaging (e.g. corneal scarring).

Diagnoses of RP were made based on clinical history, fundus examination, and full-field electroretinogram results. Most of the patients (79.5%) had non-syndromic RP, with the majority carrying a diagnosis of autosomal recessive RP (53.4%), followed by autosomal dominant (21.6%) and X-linked RP (4.5%). Syndromic RP accounted for 20.5% of the patients; of this percentage, all were diagnosed with Usher syndrome. The patients were divided into three groups according to mode of inheritance (autosomal dominant, autosomal recessive, or X-linked) with the Usher syndrome patients included in autosomal recessive subgroup.

Mutation Screening

All patients were screened for genetic mutations. DNA was extracted from whole blood with the QIAamp DNA Blood Maxi Kit 51194 (Qiagen Inc., Valencia, California, USA). ARRP genotyping micro-array (Asper Ophthalmics, Tartu, Estonia) was used to screen for 585 mutations in *CERKL*, *CNGA1*, *CNGB1*, *MERTK*, *PDE6A*, *PDE6B*, *PNR*, *RDH12*, *RGR*, *RLBP1*, *SAG*, *TULP1*, *CRB*, *RPE65*, *USH2A*, *USH3A*, *LRAT*, and *PROML1* genes; ADRP genotyping microarray (Asper Ophthalmics) was used to screen 370 mutations in *CA4*, *FSCN2*, *IMPDH1*, *NRL*, *PRPF3*, *PRPF31*, *PRPF8*, *RDS*, *RHO*, *ROM1*, *RP1*, *RP9*, *CRX*, *TOPORS*, and *PNR* genes; early onset retinal dystrophy array was used to screen for 495 disease-associated sequences in *AIPL1*, *CRB1*, *CRX*, *GUCY2D*, *LRAT*, *TULP1*, *MERTK*, *CEP290*, *RDH12*, *RP-GRIP1*, *LCA5*, and *RPE65* genes. Usher array and Bardet Biedl array (Asper Ophthalmics) were also used.

Fundus Autofluorescence

After pupil dilation, fundus autofluorescence was performed using a Spectralis HRA+OCT device (Heidelberg Engineering, Dossenheim, Germany). Fundus autofluorescence imaging

was performed with a 30° field of view, or 55° field of view if the ring was larger. The excitation wavelength was 488 nm. A 520 nm barrier filter was used to filter the emitted fluorescence light. The external boundaries of a hyperautofluorescent ring, which typically appeared better defined than the internal boundaries, were measured using the measuring tool included in the Spectralis Software. Three independent raters measured the rings' diameters across both vertical and horizontal axes (Figure 1 A, C). Intraobserver and interobserver variation among three observers were calculated, ranging from 0.51–2.38% and 0.16–8.91% of the standard deviation, respectively.

In cases involving a hyperautofluorescent arc rather than a complete ring, or a nasal edge of the ring that fell outside the optic nerve, only one axis was measured (Figure 1 B, D). The other dimension was set to "missing." Three of the 81 patients who underwent ring measurement (3.7%) displayed a high degree of asymmetry between left and right eyes despite symmetrical ERG waveforms (Figure 2). These patients were excluded from later analyses.

Statistical Analysis

Linear mixed models were used to compare vertical and horizontal diameters between three groups of inheritance patterns. A p value of<0.05 was considered statistically significant. After exclusion of seven patients with missing data in one eye and a further three with highly asymmetrical RP, 78 patients underwent bilateral symmetrical analysis. Concordance and symmetry were evaluated in the following two ways.

To estimate the association between ring diameters of the two eyes, Pearson correlation coefficients were estimated. However, additional statistical methods were needed. In a simple Pearson correlation examining the symmetries between a large group of patients' eyes, asymmetries may cancel each other out. For example, if there are an equal number of patients with more advanced disease signs in their right eyes than their left eyes, these will tend to correct one another. Thus the correlation coefficient may not reflect the true amount of variation among patient eyes. Our study attempted to identify whether those patients who displayed asymmetry failed to be detected using Pearson correlations.

We examined differences between individual eyes by looking at tendencies between patients toward asymmetry. To do so, we needed to correct for measurement error. First, the three observers were asked to measure ring diameters. The limit of agreement between the three observers was calculated with the Bland-Altman method.[34,35] First, for all vertical diameters, the limits of agreement were calculated between observers 1 and 2 (−227 to 193 um), 1 and 3 (−421 to 296 um), and 2 and 3 (−414 to 323 um). Next, for all horizontal diameters, the limits of agreement were calculated between observers 1 and 2 (−210 to 267 um), 1 and 3 (−388 to 368 um) and 2 and 3 (−412 to 342um). The highest degrees of agreement between all three observers were used as a cut-off value for the amount of measurement error that could account for symmetry, or asymmetry. Any difference between right and left eyes that fell inside the area of agreement was reported as symmetry; if the difference exceeded the highest limit of agreement, this was reported as asymmetry. Statistical analysis was performed using SAS software, version 9.2 (SAS Institute Inc, Cary, North Carolina, USA)

RESULTS

Of 88 patients, 19 had an autosomal dominant inheritance pattern (ADRP) (mean age 39 ± 18), 65 had an autosomal recessive pattern (ARRP) (mean age 36 ± 21), and four had an X-linked pattern (XLRP), (mean age 31 ± 20). Of the 65 cases classified as autosomal recessive, 18 carried a diagnosis of Usher Syndrome. All patients were screened for genetic mutations. Of the autosomal recessive patients, 17 were found to have a mutation in *USH2A*, one in *VLGR1*, two in *PDE6B*, and one in *PDE6A*. Of the autosomal dominant patients, two had a mutation in *PRPF31*, two in *RHO*, and one in *RP1*. All X-linked RP patients had *RPGR* mutations.

Best-corrected visual acuity ranged from 20/15 to 20/400 (64.4% had BCVA ≥20/30, 29.5% had BCVA 20/40 to 20/60, 6.1% had BCVA ≤ 20/70). Cystoid macular edema (CME) accounted for cases of decreased visual acuity.

Fundus Autofluorescence

All of the eyes displayed a hyperautofluorescent ring or arc on fundus autofluorescence imaging. Autofluorescence was typically normal inside the ring, except in cases that were complicated by cystoid macular edema.

Once images were collected, ring diameters were measured. In 11 out of 78 patients who were subjected to further symmetrical analysis, the horizontal diameter of the ring was impossible to measure due to an arc-like hyperfluorescence pattern, a ring larger than Spectralis's field of view, or a nasal edge of the ring falling inside of the optic nerve head area. One patient lacked a measurable vertical diameter due to obscuration of the upper ring's border by a vitreous floater.

Average ring size of all patients categorized by mode of inheritance and age group are summarized in Table 1. The mean vertical diameter of the autofluorescent ring in all patients was 3494 um. Average vertical diameters in ADRP, ARRP and XLRP patients were 3528, 3529 and 2707 um respectively; there were no systematic differences in vertical ring sizes between ADRP and ARRP ($p = 0.85$), or ADRP and XLRP ($p = 0.51$) patients. The mean horizontal diameter of autofluorescent rings for all patients was 4031 um. Average horizontal diameter in ADRP, ARRP and XLRP were 4041, 4060 and 3564 um respectively; there were no systematic differences in horizontal ring sizes between ADRP and ARRP ($p = 0.78$), or ADRP and XLRP ($p = 0.71$) patients. Factoring in age and mode of inheritance revealed that older patients seemed to have smaller rings, with each additional age predicting 24 (±SE 12, p value = 0.058) and 29 (±SE 13, p value = 0.03) um of constriction in the vertical and horizontal dimension, respectively.

Of the total of 81 patients who had AF imaging performed in both eyes, three (3.7%) were later excluded from the study due to strong asymmetry between ring sizes in left and right eyes (Figure 2). Of these three patients, two were diagnosed with ADRP with strong family history, one of them was positive for mutations in RHO, D190N, which has been described in prior studies as a cause of asymmetrical RP. The third patient was initially diagnosed with

ARRP due to lack of family history despite the negative result from ARRP mutation screening.

Among the remaining patients, correlations between the ring diameters are plotted in Figures 3 and 4. A Pearson correlation revealed a strong relationship between the vertical diameters of OD and OS eyes (r = 0.99, $p<0.0001$), and between the horizontal diameters of OD and OS eyes (r = 0.98, $p>0.0001$). Vertical and horizontal ring diameters were analyzed for bilateral concordance (Table 2). The median differences in ring diameter between OD and OS eyes were found to be 128 um (vertically) and 130 um (horizontally). The mean differences were 217 um (vertically) and 215 um (horizontally). The limits of agreement between the three observers were calculated using the Bland-Altman method. The purpose of this adjustment was to correct for measurement error due to the presence of three observers. The highest limit of agreement between the three observers was used as an upper limit for measurement error. These limits were 421 um for the vertical diameter and 412 for the horizontal diameter. Beyond this range, observer-rated differences between eyes' diameters were attributable to true asymmetry, rather than measurement error. After adjusting for potential measurement error, 85.7% and 87.3% of the patients displayed symmetrical hyperautofluorescent rings across the vertical and horizontal diameters, respectively.

DISCUSSION

The hyperautofluorescent ring in RP patients is a transitional zone between normal and abnormal retinal structures. It has been shown to correlate well with other functional and structural assessments. A strong association has been found between hyperautofluorescent ring size and preservation of the ellipsoid or IS-OS line as measured by SD-OCT; a moderate correlation has been found with pattern ERG, multifocal ERG, visual field and microperimetry (MP1) results.[4,16,17,19,21–23,25–28,30,36–39] Over longer periods, ring constriction is consistent with progressive macular dysfunction, visual field constriction, and progressive photoreceptor loss.[4,18,29]

Fundus autofluorescence is one of the most useful tools available for evaluating the natural progression of structural changes in RP. It may also be the most useful modality for measuring outcomes of therapeutic trials. Functional assessment methods, including visual fields, have the ability to detect changes in patients' visual abilities. However, functional tests have a high degree of measurement variability, even between tests performed on the same visit. In addition to the typically slow progress seen in RP patients, this variation makes it more difficult to detect small or early changes in patients.

Electroretinograms provide a more objective form of assessment. However, random variation may account for up to 20% of changes in ERGs.[40–44] In addition, as previous authors have noted, ERGs are not able to adequately measure changes in central vision. In this region, any electrical response may be related to residual normal areas of the peripheral retina that are detectable using techniques such as wide-field fundus autofluorescence. These isolated areas have been found to have preserved visual fields.[30]

In the current study, 3.7% of typical RP patients displayed highly asymmetrical autofluorescent rings. ERGs failed to show whether the left or right eye was more affected in these patients. This evidence suggests that AF imaging may be more sensitive in detecting asymmetry and progression in RP patients and would be more reliable as an outcome measurement for future gene and stem cell therapy trials, in which the contralateral eye will likely be used as a control.

The results of this study confirmed the highly bilateral structural symmetry in typical RP patients with a nearly perfect correlation coefficient ($r = 0.99$ for the vertical and $r = 0.98$ for the horizontal diameter). This is consistent with the results of Massof's visual field study, which had a high correlation coefficient ($r = 0.96$) between left and right eyes.[11] Of all patients who seemed to manifest bilateral symmetry of the hyperautofluorescent ring on clinical examination, and who, as a group, showed a Pearson correlation of 99 between left and right eyes, 14.3% and 12.7% respectively showed asymmetry across vertical and horizontal axes. In contrast, 85.7% and 87.3% displayed true symmetry between right and left eyes across vertical and horizontal diameters, respectively. Overall, when diameters were compared, the vertical diameter appeared to be a slightly better outcome measure than the horizontal, due to a higher correlation coefficient and fewer instances of missing data, especially in patients with large rings.

There were no statistical differences between ring sizes among different inheritance groups. However, among XLRP patients, there was a tendency, although not a statistically significant one, toward smaller-sized rings. This is consistent with previous studies describing XLRP as the most severe form of RP.[4,40] As expected, in our study, there was a trend showing that older patients had smaller rings.

In summary, in this study 3.7% of typical RP patients displayed highly asymmetrical hyperautofluorescent ring sizes and the majority of these patients had ADRP. The other 96.3% of typical RP patients displayed evidence of bilateral symmetry clinically; more than 85% of them were found to have highly symmetrical rings when measurement error was adjusted for. It is still in doubt whether the tendency toward symmetrical ring size, measured at one time point, implies a symmetrical rate of the progression that dates back to the beginning of the disease. By adding multiple time points, it would be possible to document whether the rate of disease progression is truly symmetrical bilaterally and to determine whether the rate of progression follows a pattern of zero-order or first-order decay. To expand on these findings, further longitudinal studies are needed.

Acknowledgments

We would like to acknowledge Jimmy Duong's contributions to our statistical analysis.

References

1. Hartong DT, Berson EL, Dryja TP. Retinitis pigmentosa. Lancet. Nov 18.2006 368:1795–1809. [PubMed: 17113430]
2. Jacobson SG, Yagasaki K, Feuer WJ, Roman AJ. Interocular asymmetry of visual function in heterozygotes of X-linked retinitis pigmentosa. Exp Eye Res. May.1989 48:679–691. [PubMed: 2737262]

3. Lee JT, Bartolomei MS. X-inactivation, imprinting, and long noncoding RNAs in health and disease. Cell. Mar 14.2013 152:1308–1323. [PubMed: 23498939]
4. Acton JH, Greenberg JP, Greenstein VC, et al. Evaluation of multimodal imaging in carriers of X-linked retinitis pigmentosa. Exp Eye Res. May 10.2013 113C:41–48. [PubMed: 23669302]
5. Mukhopadhyay R, Holder GE, Moore AT, Webster AR. Unilateral retinitis pigmentosa occurring in an individual with a germline mutation in the RP1 gene. Arch Ophthalmol. Jul.2011 129:954–956. [PubMed: 21746989]
6. Laatikainen L, Mustonen E. Asymmetry of retinitis pigmentosa-related to initial optic disc vasculitis. Acta Ophthalmologica. Aug.1992 70:543–548. [PubMed: 1414303]
7. Cogan DG. Pseudoretinitis pigmentosa. Report of two traumatic cases of recent origin. Arch Ophthalmol. Jan.1969 81:45–53. [PubMed: 5763219]
8. Lotery AJ, McBride MO, Larkin C, Sharkey JA. Pseudoretinitis pigmentosa due to sub-optimal treatment of neurosyphilis. Eye. 1996; 10:759–760. [PubMed: 9091384]
9. Sekimoto M, Hayasaka S, Noda S, Setogawa T. Pseudoretinitis pigmentosa in patients with systemic lupus erythematosus. Ann Ophthalmol. Jul.1993 25:264–266. [PubMed: 8363295]
10. Biro I. Symmetrical development of pigmentation as a specific feature of the fundus pattern in retinitis pigmentosa. Am J Ophthalmol. Jun.1963 55:1176–1179. [PubMed: 13971166]
11. Massof RW, Finkelstein D, Starr SJ, et al. Bilateral symmetry of vision disorders in typical retinitis pigmentosa. Br J Ophthalmol. Feb.1979 63:90–96. [PubMed: 311654]
12. Li Y, Tsai YT, Hsu CW, et al. Long-term safety and efficacy of human-induced pluripotent stem cell (iPS) grafts in a preclinical model of retinitis pigmentosa. Mol Med. 2012; 18:1312–1319. [PubMed: 22895806]
13. Wang NK, Tosi J, Kasanuki JM, et al. Transplantation of reprogrammed embryonic stem cells improves visual function in a mouse model for retinitis pigmentosa. Transplantation. Apr 27.2010 89:911–919. [PubMed: 20164818]
14. Wert KJ, Davis RJ, Sancho-Pelluz J, et al. Gene therapy provides long-term visual function in a pre-clinical model of retinitis pigmentosa. Human Mol Genet. Feb 1.2013 22:558–567. [PubMed: 23108158]
15. Chen RW, Greenberg JP, Lazow MA, et al. Autofluorescence imaging and spectral-domain optical coherence tomography in incomplete congenital stationary night blindness and comparison with retinitis pigmentosa. Am J Ophthalmol. Jan.2012 153:143–154. e142. [PubMed: 21920492]
16. Duncker T, Tabacaru MR, Lee W, et al. Comparison of near-infrared and short-wavelength autofluorescence in retinitis pigmentosa. Invest Ophthalmol Visual Sci. Jan.2013 54:585–591. [PubMed: 23287793]
17. Greenstein VC, Duncker T, Holopigian K, et al. Structural and functional changes associated with normal and abnormal fundus autofluorescence in patients with retinitis pigmentosa. Retina. Feb. 2012 32:349–357. [PubMed: 21909055]
18. Lima LH, Burke T, Greenstein VC, et al. Progressive constriction of the hyperautofluorescent ring in retinitis pigmentosa. Am J Ophthalmol. Apr.2012 153:718–727. e711–712. [PubMed: 22137208]
19. Lima LH, Cella W, Greenstein VC, et al. Structural assessment of hyperautofluorescent ring in patients with retinitis pigmentosa. Retina. Jul-Aug;2009 29:1025–1031. [PubMed: 19584660]
20. Lee TJ, Hwang JC, Chen RW, et al. The role of fundus autofluorescence in late-onset retinitis pigmentosa (LORP) diagnosis. Ophthalmic Genet. Jul 30.2013
21. Murakami T, Akimoto M, Ooto S, et al. Association between abnormal autofluorescence and photoreceptor disorganization in retinitis pigmentosa. Am J Ophthalmol. Apr.2008 145:687–694. [PubMed: 18242574]
22. Popovic P, Jarc-Vidmar M, Hawlina M. Abnormal fundus autofluorescence in relation to retinal function in patients with retinitis pigmentosa. Graefe's Arch Clin Exp Ophthalmol. Oct.2005 243:1018–1027. [PubMed: 15906064]
23. Wakabayashi T, Sawa M, Gomi F, Tsujikawa M. Correlation of fundus autofluorescence with photoreceptor morphology and functional changes in eyes with retinitis pigmentosa. Acta Ophthalmol. Aug.2010 88:e177–183. [PubMed: 20491687]

24. Robson AG, Egan C, Holder GE, et al. Comparing rod and cone function with fundus autofluorescence images in retinitis pigmentosa. Adv Exp Med Biol. 2003; 533:41–47. [PubMed: 15180246]
25. Robson AG, Egan CA, Luong VA, et al. Comparison of fundus autofluorescence with photopic and scotopic fine-matrix mapping in patients with retinitis pigmentosa and normal visual acuity. Invest Ophthalmol Visual Sci. Nov.2004 45:4119–4125. [PubMed: 15505064]
26. Robson AG, El-Amir A, Bailey C, et al. Pattern ERG correlates of abnormal fundus autofluorescence in patients with retinitis pigmentosa and normal visual acuity. Invest Ophthalmol Visual Sci. Aug.2003 44:3544–3550. [PubMed: 12882805]
27. Robson AG, Lenassi E, Saihan Z, et al. Comparison of fundus autofluorescence with photopic and scotopic fine matrix mapping in patients with retinitis pigmentosa: 4- to 8-year follow-up. Invest Ophthalmol Visual Sci. 2012; 53:6187–6195. [PubMed: 22899761]
28. Robson AG, Saihan Z, Jenkins SA, et al. Functional characterisation and serial imaging of abnormal fundus autofluorescence in patients with retinitis pigmentosa and normal visual acuity. Br J Ophthalmol. Apr.2006 90:472–479. [PubMed: 16547330]
29. Robson AG, Tufail A, Fitzke F, et al. Serial imaging and structure-function correlates of high-density rings of fundus autofluorescence in retinitis pigmentosa. Retina. Sep.2011 31:1670–1679. [PubMed: 21394059]
30. Schmitz-Valckenberg S, Holz FG, Bird AC, Spaide RF. Fundus autofluorescence imaging: review and perspectives. Retina. Mar.2008 28:385–409. [PubMed: 18327131]
31. Delori FC. Autofluorescence method to measure macular pigment optical densities fluorometry and autofluorescence imaging. Arch Biochem Biophys. Oct 15.2004 430:156–162. [PubMed: 15369813]
32. Delori FC, Dorey CK, Staurenghi G, et al. In vivo fluorescence of the ocular fundus exhibits retinal pigment epithelium lipofuscin characteristics. Invest Ophthalmol Visual Sci. Mar.1995 36:718–729. [PubMed: 7890502]
33. von Ruckmann A, Fitzke FW, Bird AC. Distribution of pigment epithelium autofluorescence in retinal disease state recorded in vivo and its change over time. Graefe's Arch Clin Exp Ophthalmol. Jan.1999 237:1–9. [PubMed: 9951634]
34. Bland JM, Altman DG. Measuring agreement in method comparison studies. Statistical Meth Med Res. Jun.1999 8:135–160.
35. Steinberg JS, Auge J, Jaffe GJ, et al. Longitudinal analysis of reticular drusen associated with geographic atrophy in age-related macular degeneration. Investigat Ophthalmol Visual Sci. Jun. 2013 54:4054–4060.
36. Aizawa S, Mitamura Y, Hagiwara A, et al. Changes of fundus autofluorescence, photoreceptor inner and outer segment junction line, and visual function in patients with retinitis pigmentosa. Clin Exp Ophthalmol. Aug.2010 38:597–604.
37. Fakin A, Jarc-Vidmar M, Glavac D, et al. Fundus autofluorescence and optical coherence tomography in relation to visual function in Usher syndrome type 1 and 2. Vision Res. Dec 15.2012 75:60–70. [PubMed: 23000274]
38. Fleckenstein M, Charbel Issa P, Fuchs HA, et al. Discrete arcs of increased fundus autofluorescence in retinal dystrophies and functional correlate on microperimetry. Eye. Mar.2009 23:567–575. [PubMed: 18344954]
39. Oishi A, Ogino K, Makiyama Y, et al. Wide-field fundus autofluorescence imaging of retinitis pigmentosa. Ophthalmology. Sep.2013 120:1827–1834. [PubMed: 23631947]
40. Birch DG, Anderson JL, Fish GE. Yearly rates of rod and cone functional loss in retinitis pigmentosa and cone-rod dystrophy. Ophthalmology. Feb.1999 106:258–268. [PubMed: 9951474]
41. Grover S, Fishman GA, Birch DG, et al. Variability of full-field electroretinogram responses in subjects without diffuse photoreceptor cell disease. Ophthalmology. Jun.2003 110:1159–1163. [PubMed: 12799241]
42. Fishman GA, Chappelow AV, Anderson RJ, et al. Short-term inter-visit variability of erg amplitudes in normal subjects and patients with retinitis pigmentosa. Retina. Dec.2005 25:1014–1021. [PubMed: 16340532]

43. Jacobi PC, Miliczek KD, Zrenner E. Experiences with the international standard for clinical electroretinography: normative values for clinical practice, interindividual and intraindividual variations and possible extensions. Documenta Ophthalmologica/Adv Ophthalmol. 1993; 85:95–114.

44. Ross DF, Fishman GA, Gilbert LD, Anderson RJ. Variability of visual field measurements in normal subjects and patients with retinitis pigmentosa. Arch Ophthalmol. Jul.1984 102:1004–1010. [PubMed: 6743076]

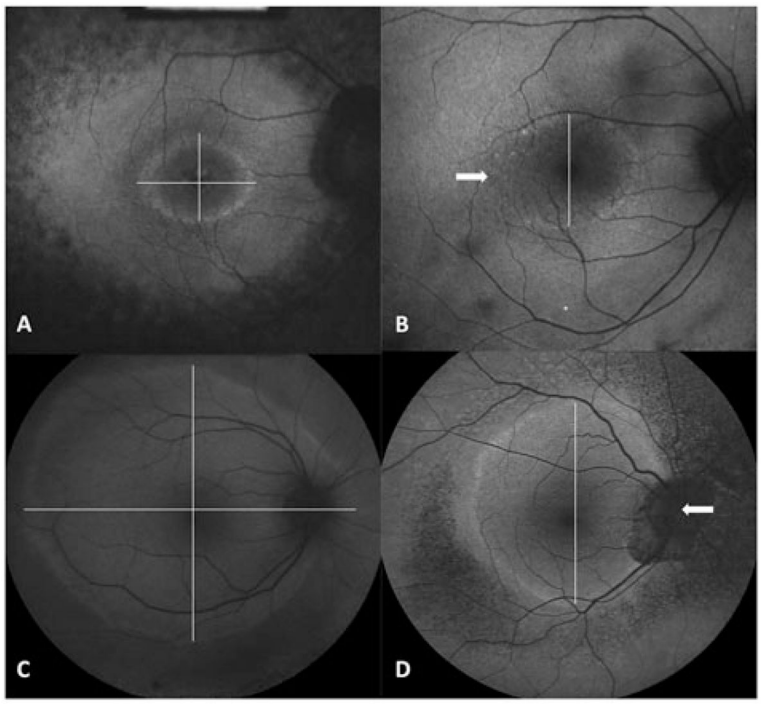

FIGURE 1.

Hyperautofluorescent rings from AF imaging. (A, C) Vertical and horizontal measurement at the largest dimension of high density ring outer border. (B, D) Example of two patients in whom the horizontal diameters were set to missing due to an inability to define the ring outer border. Arrows highlight the poorly defined ring area.

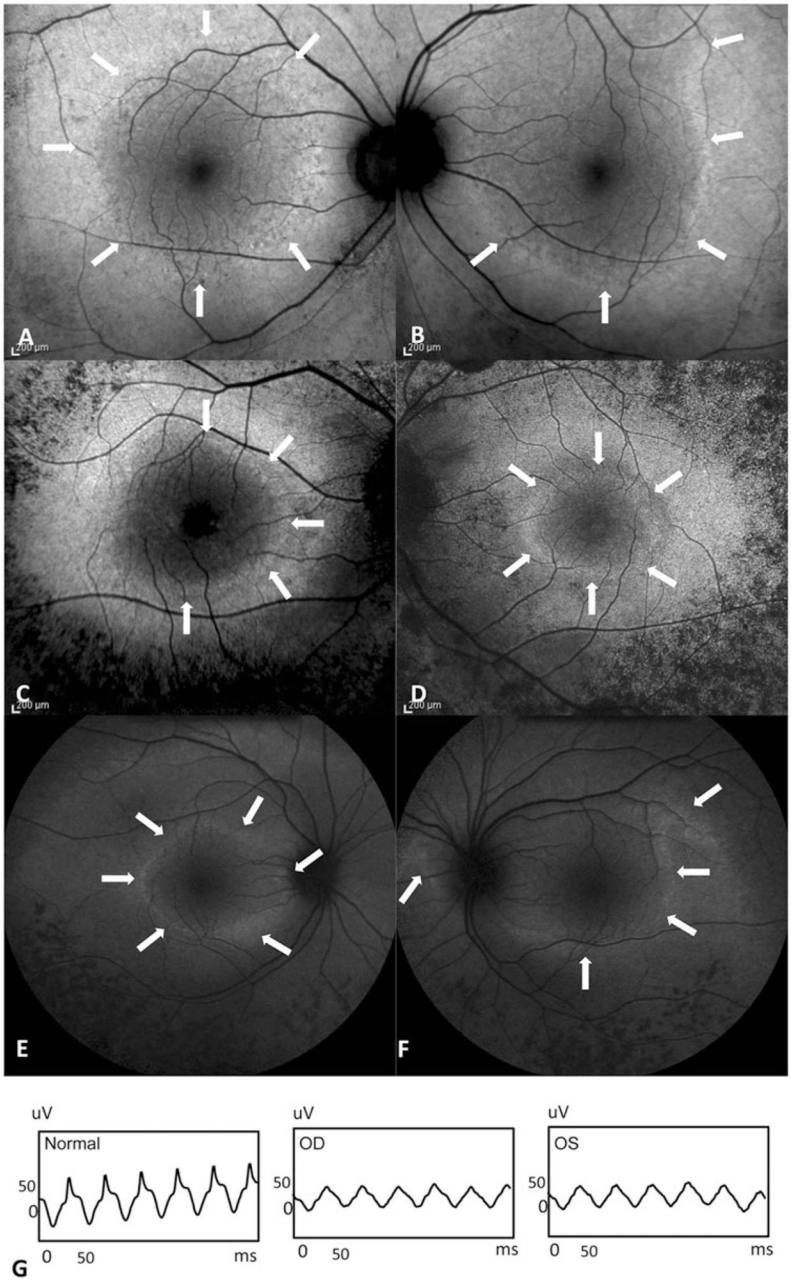

FIGURE 2.

Fundus autofluorescence of three patients with asymmetrical ring. Arrows highlight the asymmetrical area. (A, B) This patient was diagnosed with ARRP. (C, D) Patient with strong family history of ADRP, unknown mutation. (E, F) RHO D190N mutation patient with ADRP family history. (G) Representative 30 Hz flicker electroretinogram showed similar voltage and waveform despite asymmetrical hyperautofluorescence ring of RHO D190N patient.

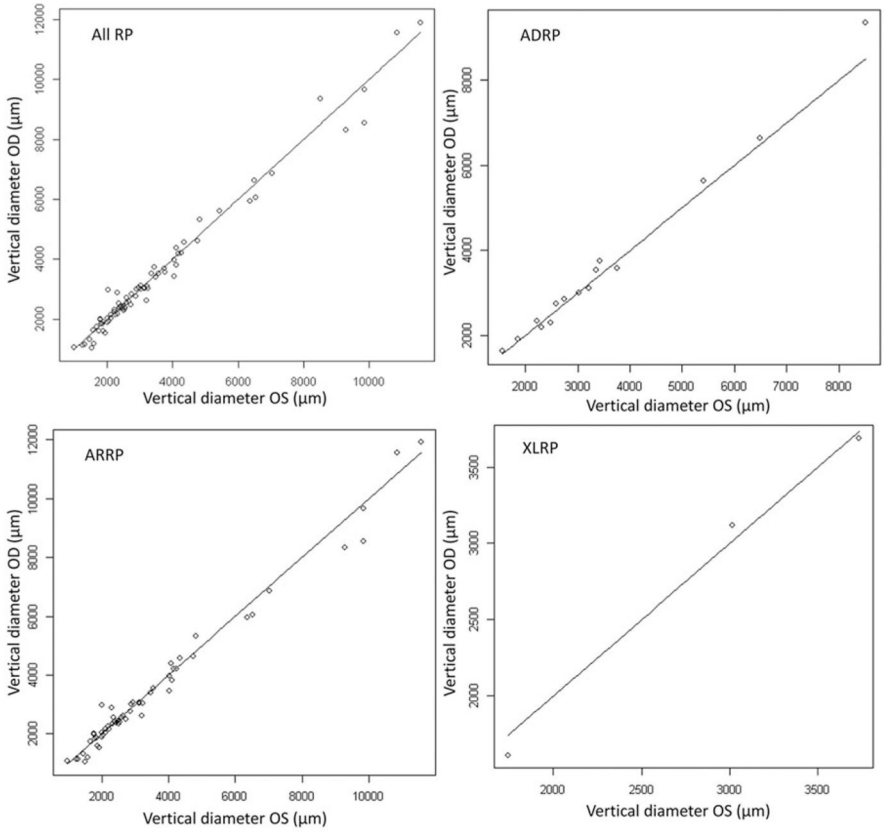

FIGURE 3.

The scatter plot of vertical diameters showed correlation between the right and left eyes of all RP patients (ADRP, ARRP and XLRP). The correlation coefficient between both eyes was 0.99 with a *p* value <0.001.

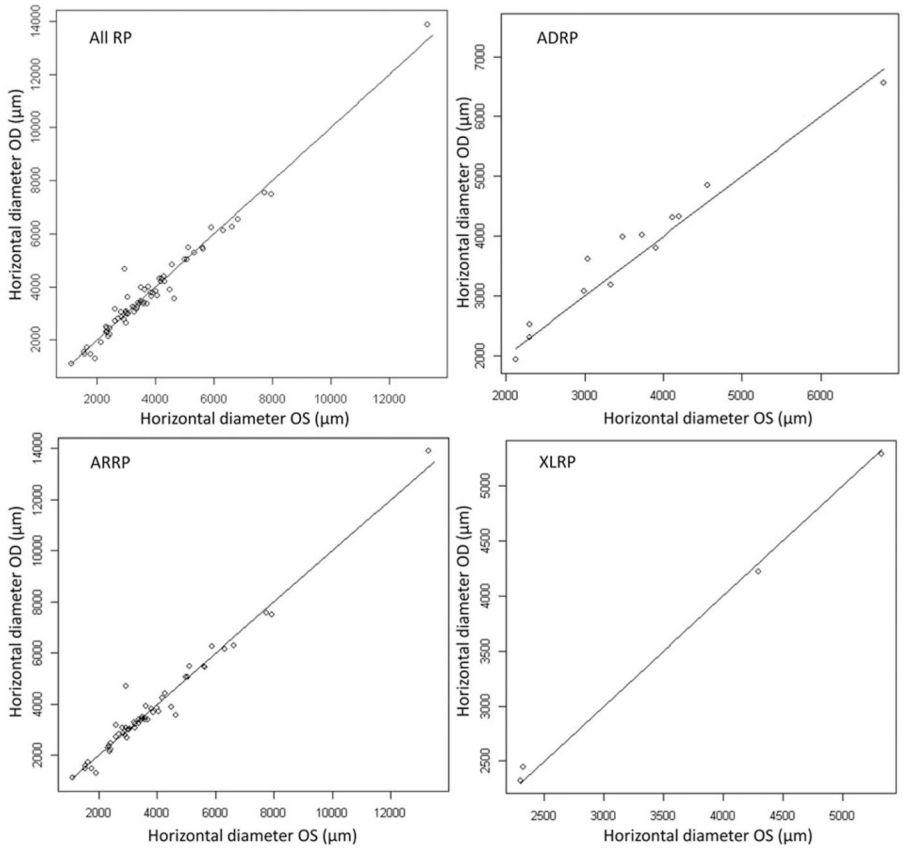

FIGURE 4.

The scatter plot of horizontal diameter showed correlation between the right and left eyes of all RP patients (ADRP, ARRP and XLRP). The correlation coefficient between both eyes was 0.98 with a *p* value <0.001.

TABLE 1

Average ring size of all patients categorized by mode of inheritance and age group.

				Mean vertical diameter (range in um)					
Diagnosis	**Patients**	**Eyes**	**Mean age**	**All ages (100%)**	**0–20 years (26.14%)**	**21–40 years (32.95%)**	**41–60 years (30.68%)**	**61–80 years (7.95%)**	**81–100 years (2.27%)**
Total	88	165	36.7						
ADRP	19	34	39.08	3528(1557–9354)	3270(2297–4907)	3454(1557–6645)	3888(1863–9354)	2704(2583–2796)	–
ARRP	65	124	36.31	3529(972–11912)	4462(1151–11912)	3573(1037–11569)	2742(972–7032)	3083(1541–5971)	2814(1786–4041)
XLRP	4	7	31.67	2707(1609–3733)	3711(3690–3733)	2372(1609–3120)	2040(2040–2040)	–	–

				Mean horizontal diameter (range in um)					
Diagnosis	**Patients**	**Eyes**	**Mean age**	**All ages**	**0–20 years**	**21–40 years**	**41–60 years**	**61–80 years**	**81–100 years**
Total	88	158	36.7						
ADRP	19	32	39.08	4041(1931–10255)	4884(3183–10255)	3761(1931–7497)	3828(2303–6799)	3485(3043–3787)	–
ARRP	65	118	36.31	4060(1106–13894)	4811(1547–13894)	4127(1310–13475)	3460(1106–7939)	3885(2148–6543)	3298(2611–3992)
XLRP	4	8	31.67	3564(2300–5324)	5306(5287–5324)	3283(2300–4291)	2386(2325–2447)	–	–

Table 2

Differences in hyperautofluorescent ring size between right and left eyes in patients with typical retinitis pigmentosa.

	Patients	OD	OS	Mean of the difference ± SD	Median	Lower quartile (Q1)	Upper quartile (Q3)	Min	Max
Vertical diameter (um)									
Total	77	3537 (972–11564)	3411 (1037–11912)	217 ± 246.5	128	66	247	4	1290
ADRP	15	3486 (1557–8512)	3576 (1623–9354)	186.8 ± 195.6	149	98	193	13	841
ARRP	59	3646 (972–11564)	3408 (1037–11912)	230.9 ± 262.8	128	56	287	4	1290
XLRP	3	2831 (1743–3733)	2615 (1609–3690)	93.11 ± 45.9	103	43	133	43	133
Horizontal diameter (um)									
Total	71	4100 (1106–13475)	3797 (1110–13894)	214.6 ± 266.8	130	52	278	3	1748
ADRP	13	3723 (2123–6799)	4360 (1931–10255)	229.8 ± 160.9	197	135	278	3	581
ARRP	54	4301 (1106–13475)	3811 (1110–13894)	222.1 ± 293.6	124	47	291	4	1748
XLRP	4	3560 (2300–5324)	3569 (2325–5287)	64.59 ± 43.57	56	31	98	25	122